Electronic Supporting Information

Quercetin@Gd^{3+} doped Prussian blue nanocube induces pyroptotic death of MDA-MB-231 cells: combinational targeted multimodal therapy, dual modal MRI, intuitive modelling of r_1-r_2 relaxivities

Panchanan Sahoo[†,‡], Pulak Jana[§,†], Sudip Kundu[†], Snehasis Mishra[†], Krishnananda Chattopadhyay[§], Abhishek Mukherjee[#,‡], Chandan Kumar Ghosh[*,†]

[†]School of Materials Science and Nanotechnology, Jadavpur University, Kolkata-700032, India

[‡]Agricultural and Ecological Research Unit, Biological Science Division, Indian Statistical Institute, Giridih, Jharkhand, India

[§]Structural Biology & Bio-Informatics Division, CSIR-Indian Institute of Chemical Biology, 4, Raja S. C. Mallick Road, Kolkata 700032, India

[†]Academy of Scientific and Innovative Research (AcSIR), Ghaziabad, Uttar Pradesh-201002, India

Calculation of the photothermal conversion efficiency:

One of the most extensively used equation to determine photothermal conversion efficiency of PB, GPB and GPBA nanocubes (NC) under 808 nm (5.26 W·cm^{-2}, total power 1 W) laser irradiation is described as follows:[1,2]

$$\eta = \frac{hA(T_{max} - T_{sur}) - Q_w}{I(1 - 10^{-A_{808}})} \quad \text{(S1)}$$

Where h and A are the heat transfer coefficient and surface area of the quartz cuvette in which aqueous solution of the NC samples have been exposed under irradiation; T_{max} is steady state temperature of the NC aqueous solution; T_{sur} is the surrounding temperature; Q_w is associated with the converted energy by quartz cuvette contained only aqueous solution from radiant energy which is determined to be 8.4 mW; I is the power of incident NIR laser beam and A_{808} is the absorbance of the particular NC sample at a wavelength of 808 nm.

Herein, to find out hA value, a dimensionless force temperature (θ) has been introduced which is associated with the T_{max}.

$$\theta = \frac{T - T_{sur}}{T_{max} - T_{sur}} \quad \text{(S2)}$$

And another parameter known as time constant related to the NC sample is defined as

$$\tau_s = \frac{\sum_i m_i c_{pi}}{hA} \quad \text{(S3)}$$

Where, $\sum_i m_i c_{pi}$ is the product of mass and heat capacity of quartz cuvette, NC sample and solvent in the system. Thus, τ_s can be calculated from the following equation by considering cooling period of the solution:

$$t = -\tau_s ln\theta \quad \text{(S4)}$$

Then, η can be intended after findings hA value followed by equation S1.

Figure S4(a-e) represents linear plot between cooling period (t) and -lnθ with slope τ_s to be 562.46, 585.47, 557.09, 608.43 and 688.59 s corresponding to PB, $GPB_{0.25}$, $GPB_{0.5}$, $GPB_{0.75}$ and GPBA respectively. Finally, photothermal conversion efficiency is calculated to be 33.85, 51.25, 65.56, 51.45 and 35.49% respectively.

Table S1: Feeding amounts of reactants during synthesis in Solution A

Sample Name	$FeCl_3.6H_2O$ (mmol)	$Gd(NO_3)_3.6H_2O$ (mmol)
PB	0.0198	0.00
$GPB_{0.25}$	0.0148	0.0049
$GPB_{0.50}$	0.0099	0.0099
$GPB_{0.75}$	0.0049	0.0148
GPBA	0.00	0.0198

Table S2: Variation in the occupancy probability of the different atoms in the unit cell structure of PB, GPB and GPBA as obtained by Rietveld analysis using the Maud software

Atom	**site**	**PB**, R_p=18.68, R_{wp}=15.71		**$GPB_{0.25}$**, R_p=16.55, R_{wp}=13.42	
		Position (x)	**Occupancy**	**Position (x)**	**Occupancy**
Fe^{3+}	1a	0.0	1.0	0.0	0.7732842(20)
	3c	0.0	1.0	0.0	0.9133229(8)
Fe^{2+}	1b	0.50486345(9)	**0.6592583(21)**	0.5	**0.75717217(23)**
	3d	0.5002564(13)	0.7803208(17)	0.5	0.8512476(11)
N	6e	0.20095892(5)	0.7803186(23)	0.21973883(21)	0.6524139(17)

	6f	0.20777132(6)	0.6590573(8)	0.19607785(19)	0.68172204(26)
	12h	0.3086982(18)	0.7803359(19)	0.29398748(9)	0.7618029(9)
C	6e	0.31160247(2)	0.7803157(12)	0.2527187(13)	0.7553462(21)
	6f	0.2108135(8)	0.6592680(10)	0.3369625(17)	0.5803227(25)
	12h	0.19350913(21)	0.7803082(13)	0.24345358(7)	0.8885231(11)
O	6e	0.20546116(6)	0.2196236(24)	0.28894728(15)	0.20116886(13)
	6f	0.31103197(8)	0.3418713(15)	0.19607785(8)	0.3532405(20)
	12h	0.21343586(11)	0.2196520(17)	0.2519634(13)	0.19178203(6)
O	8g	0.28311816(7)	0.9769835(23)	0.24846497(4)	1.0557612(3)
Gd^{3+}	1a	0.0		0.0	0.2878626(8)
	3c	0.0		0.0	0.024392676(3)

Atom	**site**	**$GPB_{0.50}$,** R_p=18.01, R_{wp}=16.70		**$GPB_{0.75}$,** R_p=15.01, R_{wp}=12.36	
		Position (x)	**Occupancy**	**Position (x)**	**Occupancy**
Fe^{3+}	1a	0.0	0.19958599(6)	0.0	0.04379456(3)
	3c	0.0	0.6955486(7)	0.0	0.22820742(4)
Fe^{2+}	1b	0.5	**0.8748906(7)**	0.5	**0.8925268(5)**
	3d	0.5	0.72967404(6)	0.5	0.6744579(10)
N	6e	0.24126482(11)	0.29024577(8)	0.22482389(5)	0.34185156(28)
	6f	0.22089453(8)	0.87297755(11)	0.20800404(2)	0.935618(11)
	12h	0.2812284(9)	0.7125842(7)	0.29865497(1)	0.83086663(13)
C	6e	0.28790888(17)	0.711003(9)	0.23690972(1)	0.96722984(22)
	6f	0.3432895(12)	0.8710056(7)	0.3080017(2)	0.96336(15)
	12h	0.17622626(8)	0.7115617(6)	0.19111414(1)	0.93343514(14)
O	6e	0.26116607(16)	0.29032323(6)	0.22464009(3)	0.36714977(9)
	6f	0.21971194(21)	0.13004822(4)	0.2045692(3)	0.083756045(7)
	12h	0.2779372(7)	0.2905587(4)	0.2578505(1)	0.36965746(6)
O	8g	0.27506152(13)	0.98139584(8)	0.27008986(1)	0.9853173(17)
Gd^{3+}	1a	0.0	0.7909804(8)	0.0	0.8079837(13)
	3c	0.0	0.29800105(2)	0.0	0.60148686(9)
	3c	0.0	0.29800105(2)	0.0	0.60148686(9)

Atom	**site**	**GPBA**, R_p=11.75, R_{wp}=14.95	
		Position (x)	**Occupancy**

Gd^{3+}	1a	0.0	1
	3c	0.0	1
Fe^{2+}	1b	0.5	**0.40191638(8)**
	3d	0.5	0.8972872(5)
N	6e	0.28806(14)	0.8323061(12)
	6f	0.43577(17)	0.31923234(17)
	12h	0.3258(7)	0.9944583(14)
C	6e	0.27169(21)	0.9518085(8)
	6f	0.43577(4)	0.37184647(2)
	12h	0.19898(6)	0.878701(3)
O	6e	0.57235(11)	0.1460648(6)
	6f	0.43577(14)	0.6850089(12)
	12h	0.86476(9)	0.17641485(15)
O	8g	0.28206(3)	0.97429556(4)

Table S3: Elemental analysis as obtained from FESEM-EDX measurement

Sample	at% of Fe	at% of Gd	at% of N
$GPB_{0.25}$	28.60	0.05	42.67
$GPB_{0.50}$	23.47	0.35	52.19
$GPB_{0.75}$	12.81	0.43	73.31
GPBA	10.81	1.21	66.37

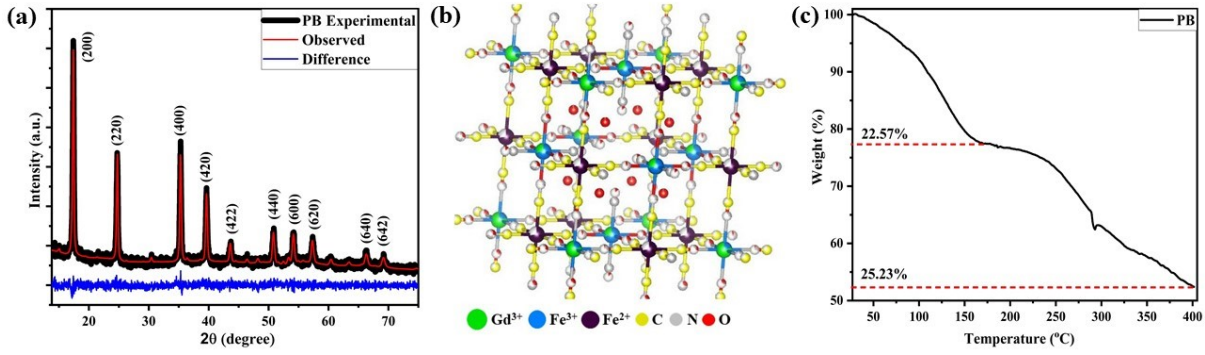

Fig. S1: (a)Reitveld refinement of PB XRD pattern with difference between experimental and refined patterns. (b) Unit cell structure of representative $GPB_{0.50}$ nanocube. (c) TGA plot of PB.

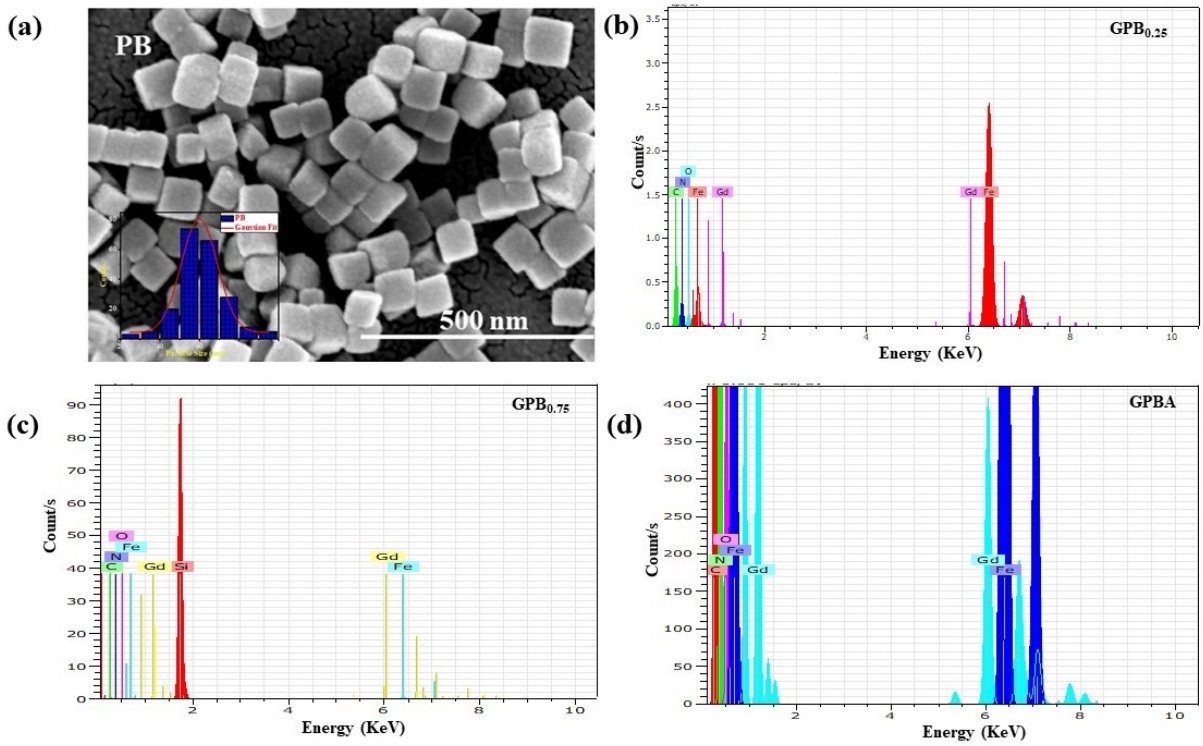

Fig. S2: (a) FESEM image and size distribution histogram in the inset of PB nanocubes. EDX spectrum of (b) $GPB_{0.25}$, (c) $GPB_{0.50}$ and (d) GPBA nanocubes.

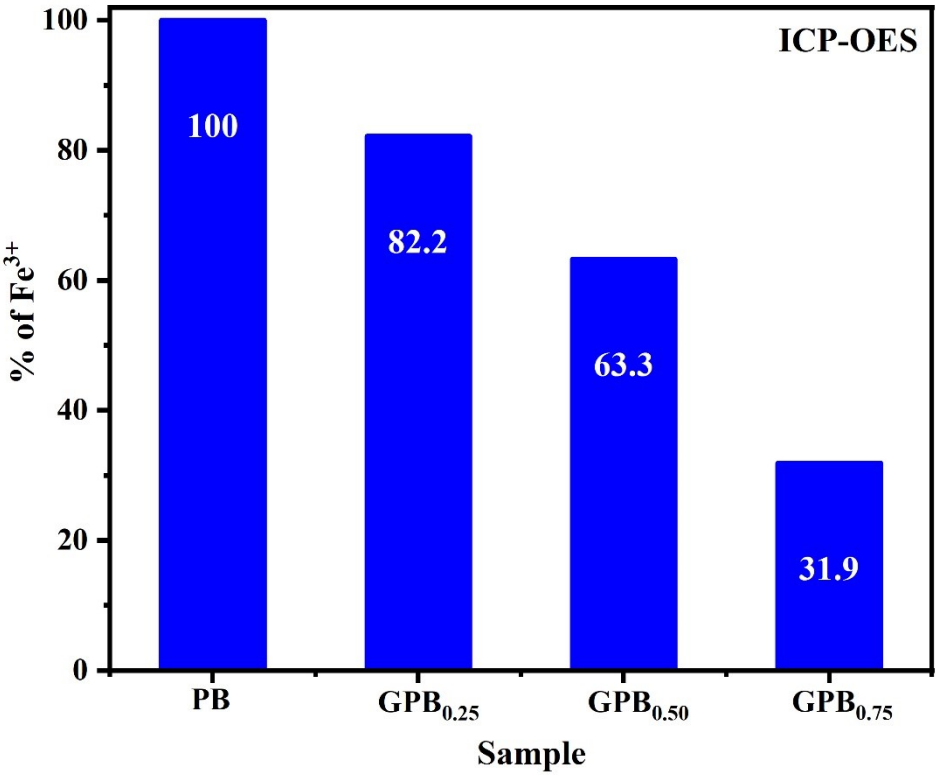

Fig. S3: ICP-OES measurement to find percentage Fe^{3+} content in bare PB and GPB samples (initial concentration of exposed samples was 40 µg/mL).

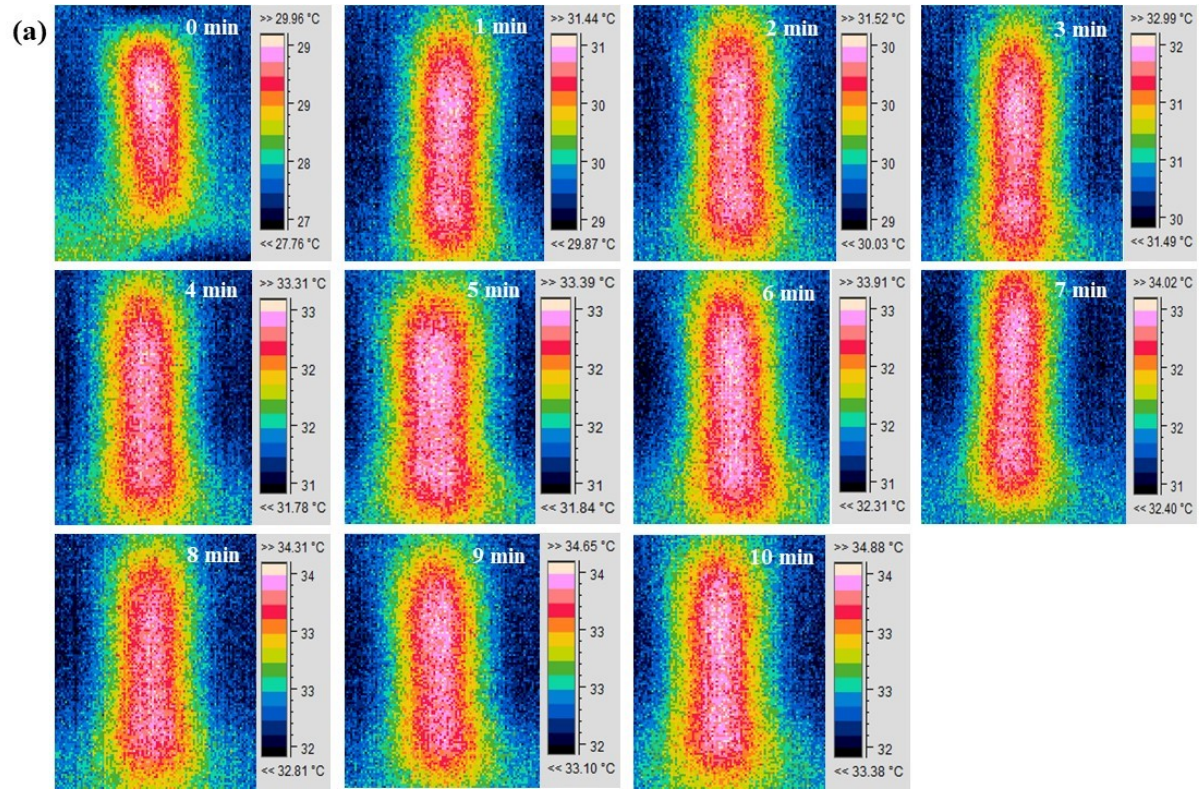
(a)
0 min
>> 29.96 °C
<< 27.76 °C
1 min
>> 31.44 °C
<< 29.87 °C
2 min
>> 31.52 °C
<< 30.03 °C
3 min
>> 32.99 °C
<< 31.49 °C
4 min
>> 33.31 °C
<< 31.78 °C
5 min
>> 33.39 °C
<< 31.84 °C
6 min
>> 33.91 °C
<< 32.31 °C
7 min
>> 34.02 °C
<< 32.40 °C
8 min
>> 34.31 °C
<< 32.81 °C
9 min
>> 34.65 °C
<< 33.10 °C
10 min
>> 34.88 °C
<< 33.38 °C

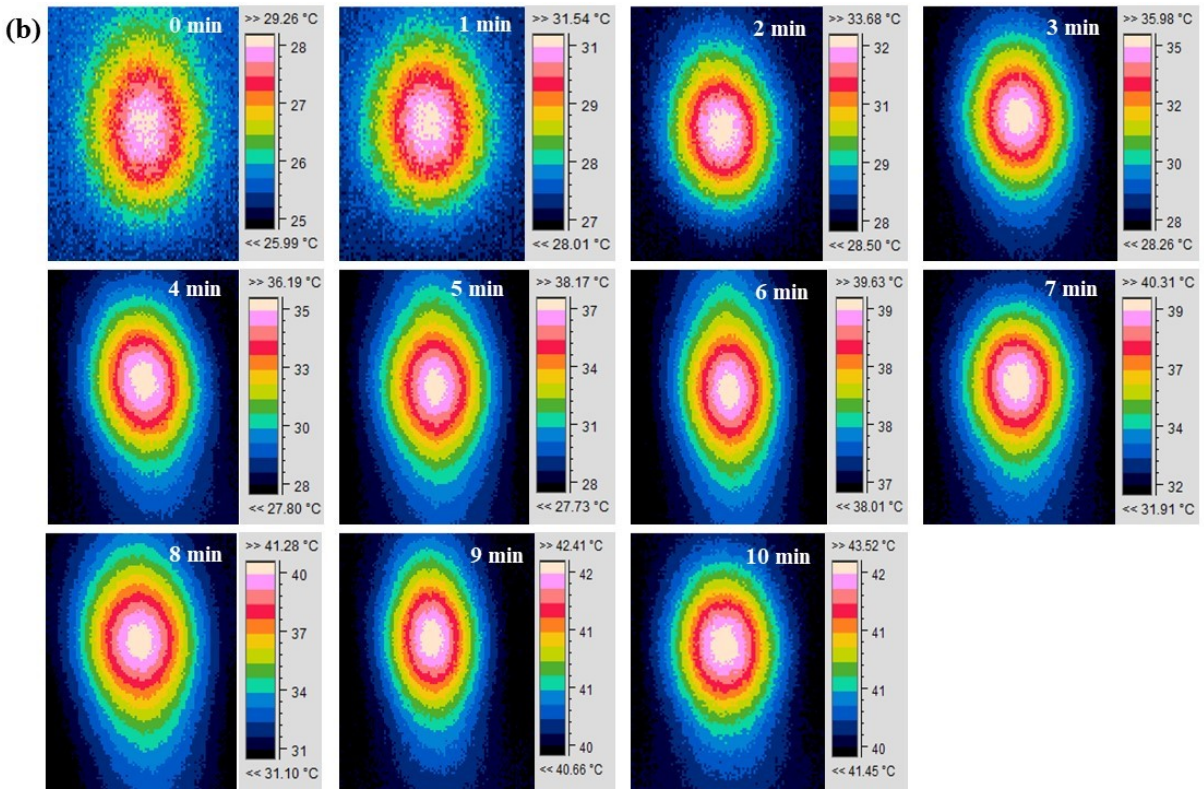
(b)
0 min
>> 29.26 °C
<< 25.99 °C
1 min
>> 31.54 °C
<< 28.01 °C
2 min
>> 33.68 °C
<< 28.50 °C
3 min
>> 35.98 °C
<< 28.26 °C
4 min
>> 36.19 °C
<< 27.80 °C
5 min
>> 38.17 °C
<< 27.73 °C
6 min
>> 39.63 °C
<< 38.01 °C
7 min
>> 40.31 °C
<< 31.91 °C
8 min
>> 41.28 °C
<< 31.10 °C
9 min
>> 42.41 °C
<< 40.66 °C
10 min
>> 43.52 °C
<< 41.45 °C

(c)

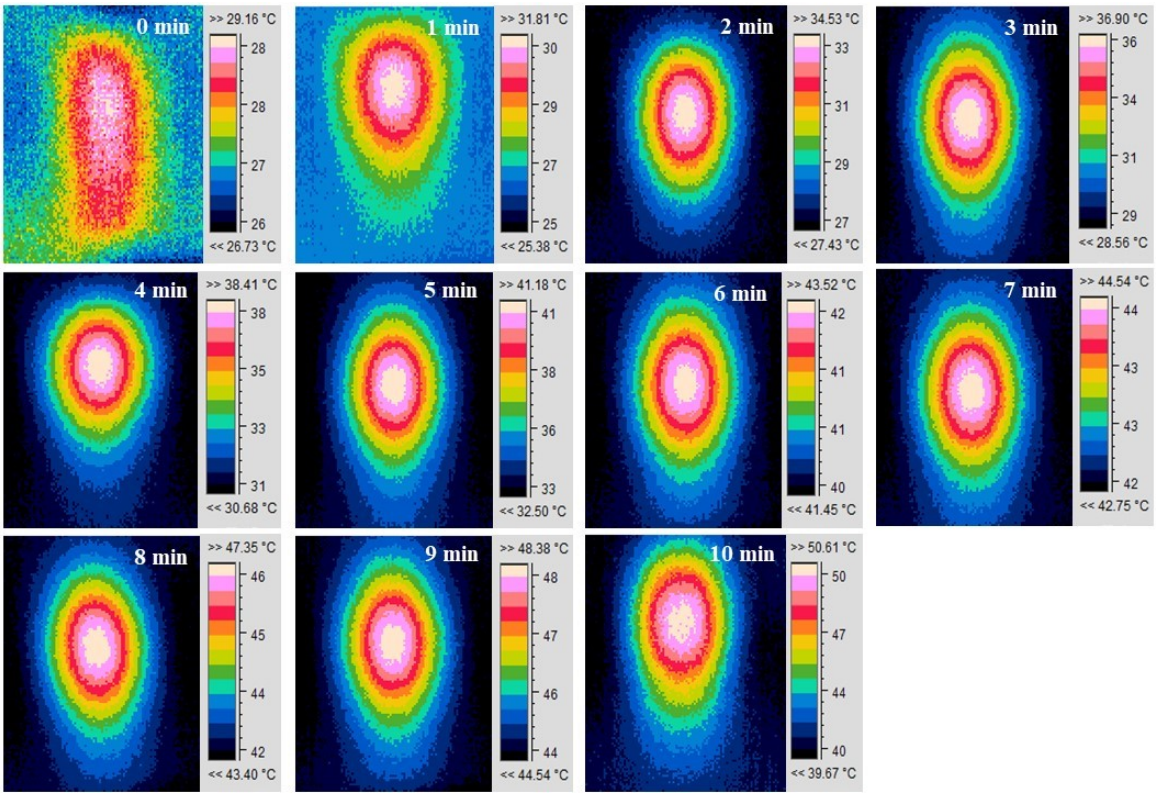
0 min
>> 29.16 °C
28
28
27
26
<< 26.73 °C
1 min
>> 31.81 °C
30
29
27
25
<< 25.38 °C
2 min
>> 34.53 °C
33
31
29
27
<< 27.43 °C
3 min
>> 36.90 °C
36
34
31
29
<< 28.56 °C
4 min
>> 38.41 °C
38
35
33
31
<< 30.68 °C
5 min
>> 41.18 °C
41
38
36
33
<< 32.50 °C
6 min
>> 43.52 °C
42
41
41
40
<< 41.45 °C
7 min
>> 44.54 °C
44
43
43
42
<< 42.75 °C
8 min
>> 47.35 °C
46
45
44
42
<< 43.40 °C
9 min
>> 48.38 °C
48
47
46
44
<< 44.54 °C
10 min
>> 50.61 °C
50
47
44
40
<< 39.67 °C

(d)

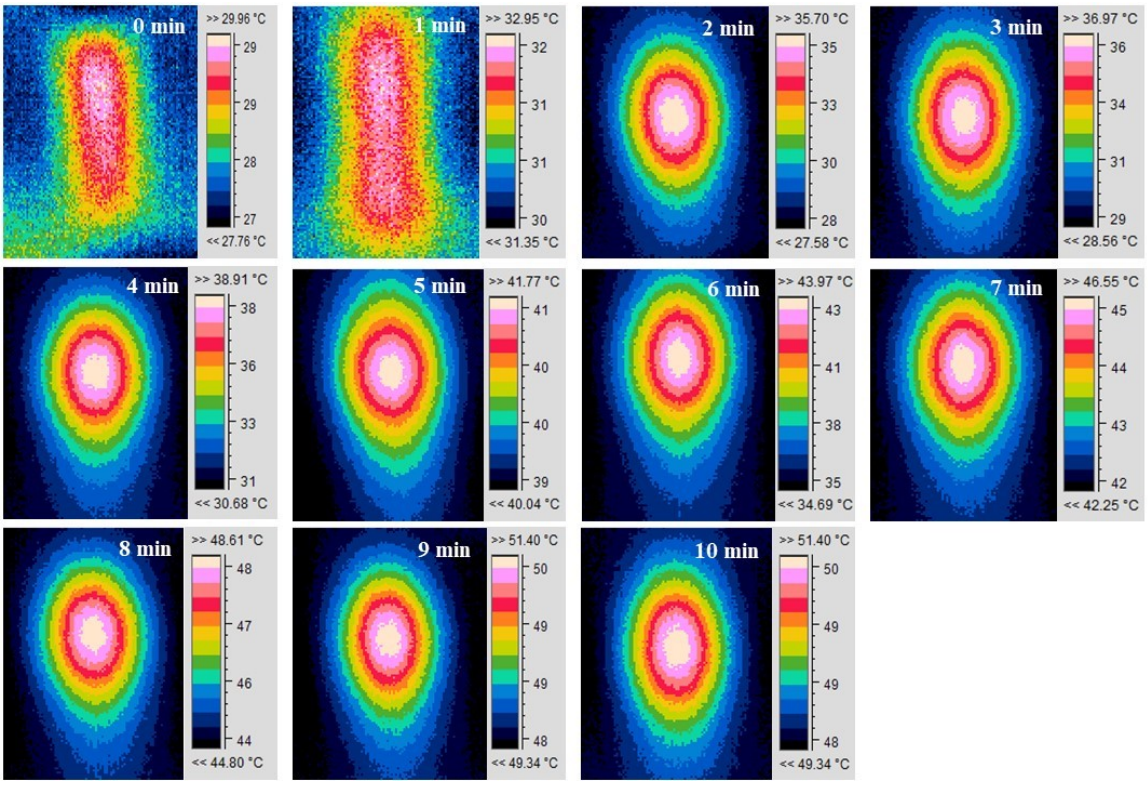
0 min
>> 29.96 °C
29
29
28
27
<< 27.76 °C
1 min
>> 32.95 °C
32
31
31
30
<< 31.35 °C
2 min
>> 35.70 °C
35
33
30
28
<< 27.58 °C
3 min
>> 36.97 °C
36
34
31
29
<< 28.56 °C
4 min
>> 38.91 °C
38
36
33
31
<< 30.68 °C
5 min
>> 41.77 °C
41
40
40
39
<< 40.04 °C
6 min
>> 43.97 °C
43
41
38
35
<< 34.69 °C
7 min
>> 46.55 °C
45
44
43
42
<< 42.25 °C
8 min
>> 48.61 °C
48
47
46
44
<< 44.80 °C
9 min
>> 51.40 °C
50
49
49
48
<< 49.34 °C
10 min
>> 51.40 °C
50
49
49
48
<< 49.34 °C

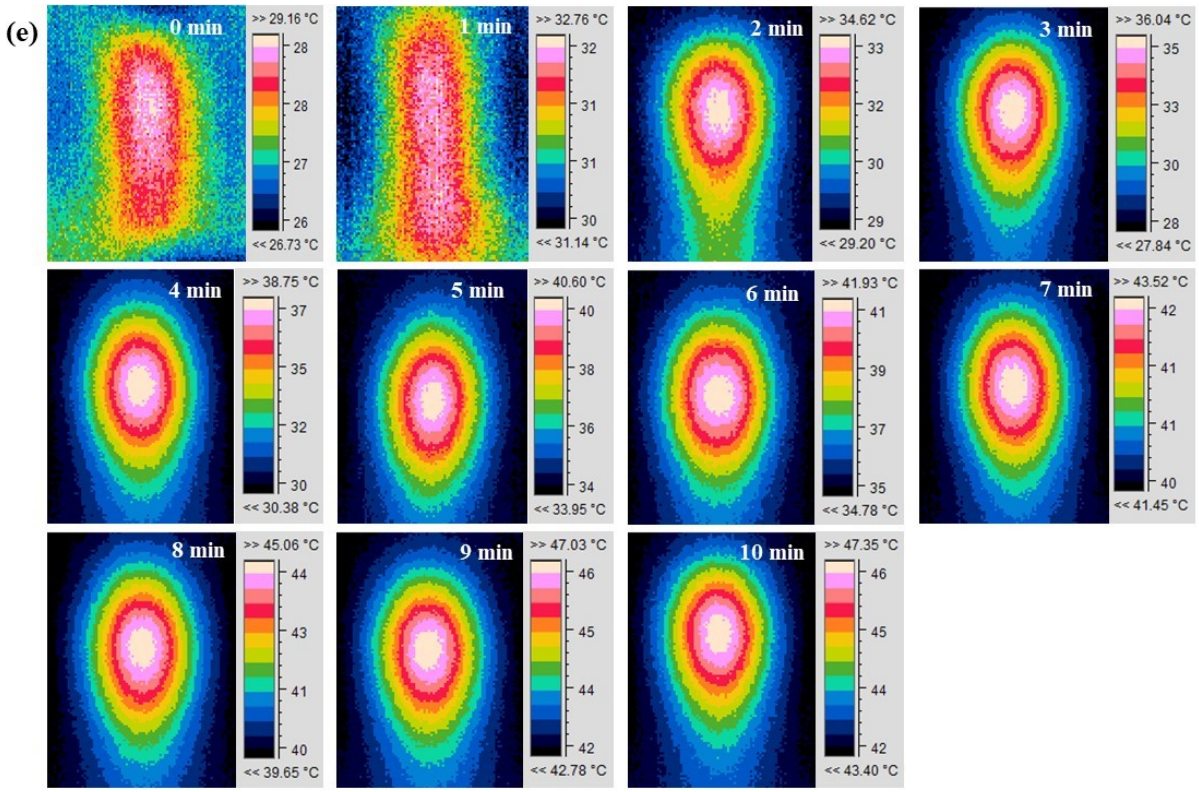

Fig. S4: Thermographs of (a) DI, (b) PB, (c) $GPB_{0.25}$, (d) $GPB_{0.75}$, (e) GPBA nanocubes sample under 808 nm NIR laser irradiation over 10 minutes.

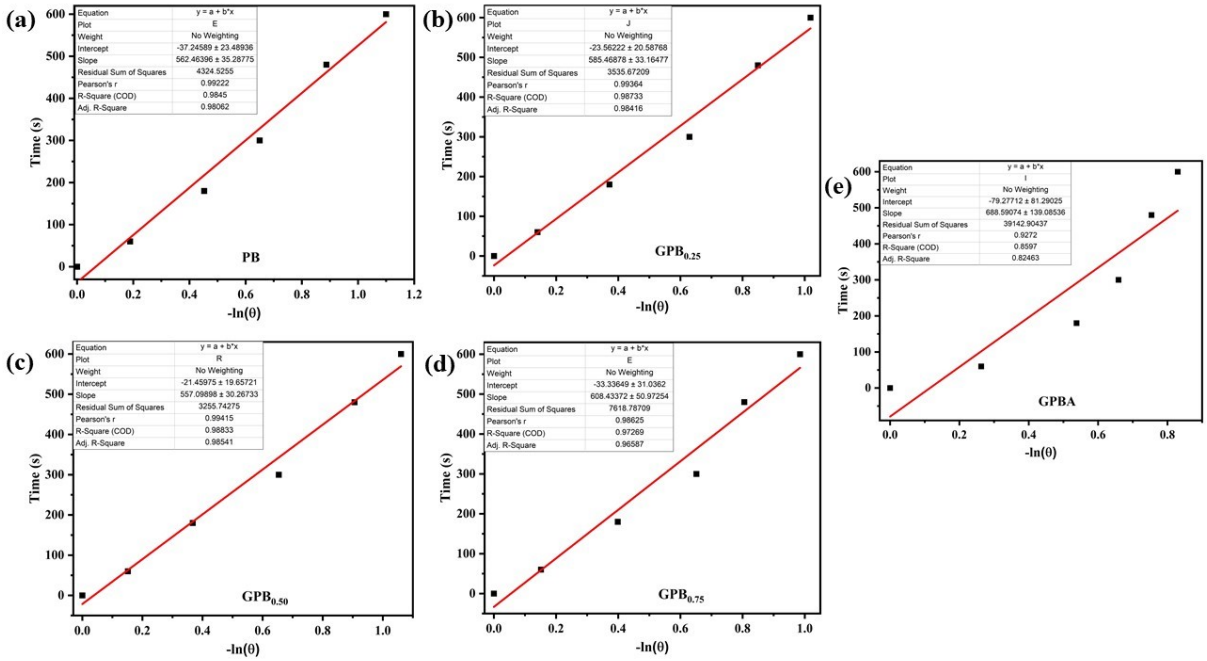

Fig. S5: Plot and linear fit of time versus negative natural logarithm of the temperature

increment for the cooling rate of (a) PB, (b) $GPB_{0.25}$, (c)$GPB_{0.50}$, (d) $GPB_{0.75}$ and (e) GPBA under 808 nm laser.

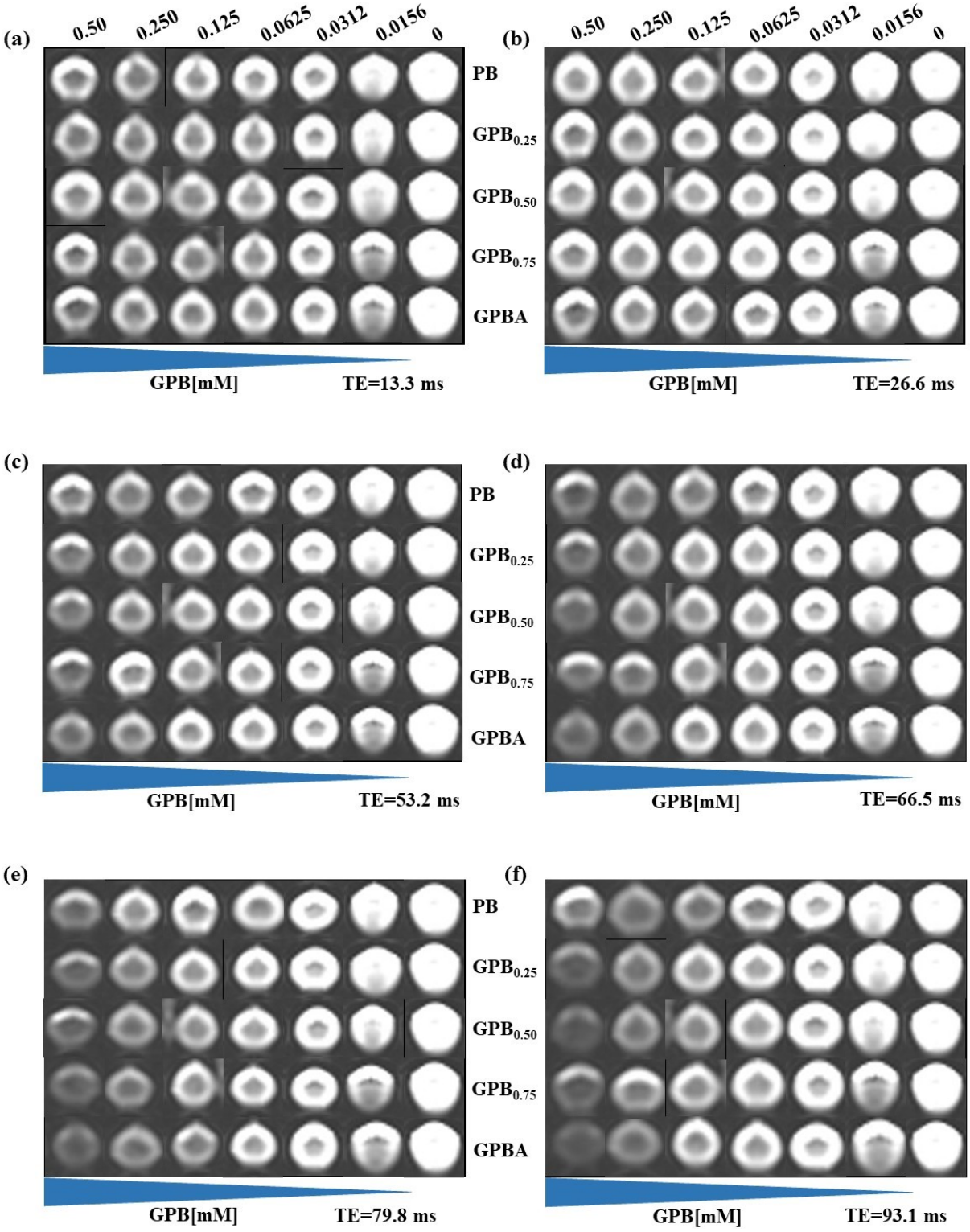

Fig. S6: Concentration dependant T_2 weighted MR images at 3 T showing hypo intensity from PB, $GPB_{0.25}$, $GPB_{0.50}$, $GPB_{0.75}$ and GPBA using spin-echo sequences with TR: 1770 ms

and variable TE of (a) 13.3 ms, (b) 26.6 ms, (c) 53.2 ms, (d) 66.5 ms, (e) 79.8 ms and (f) 93.1 ms.

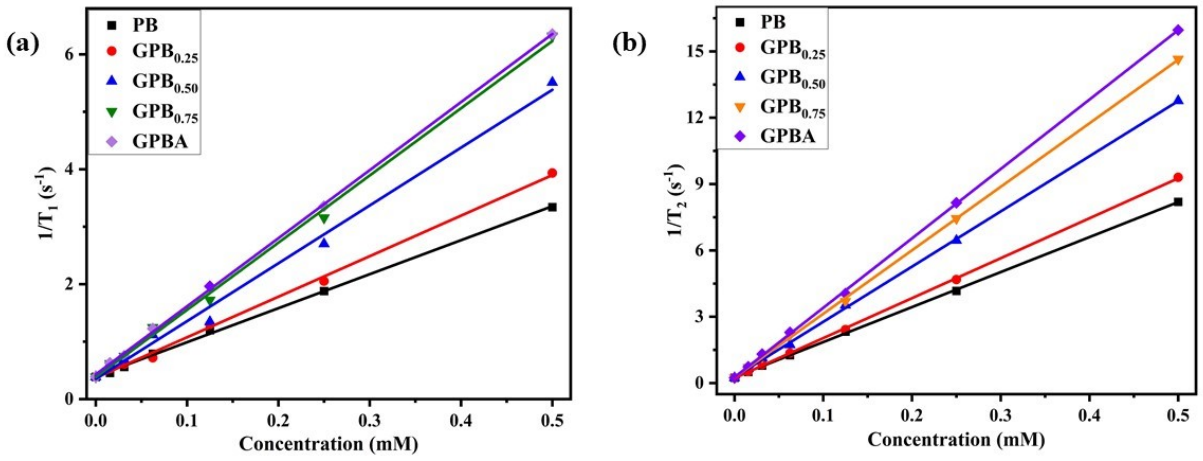

Fig. S7: Concentration dependent (a) T_1 and (b) T_2 relaxation rates. The relaxivities values were determined to be r_1 ~ 5.91, 7.05, 10.06, 11.69 11.84 $mM^{-1}s^{-1}$ and r_2 ~ 15.82, 18.07, 24.96, 28.72 31.39 $mM^{-1}s^{-1}$.

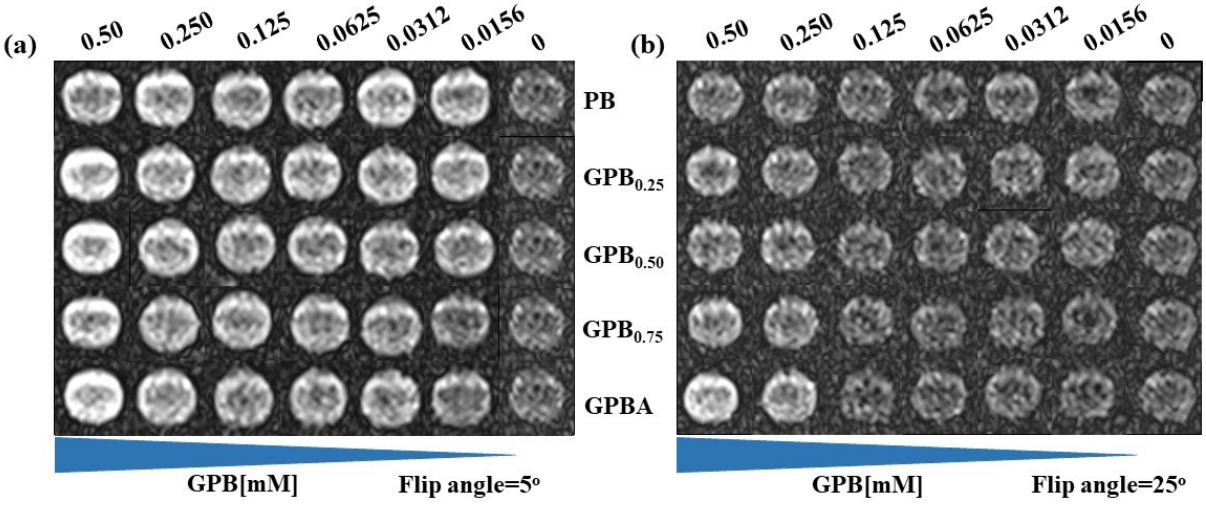

Fig. S8: Concentration dependant T_1 weighted MR images at 3 T showing brightening effect from PB, $GPB_{0.25}$, $GPB_{0.50}$, $GPB_{0.75}$ and GPBA using 3D gradient spin-echo sequences with TR: 15 ms, TE: 2.71 ms and variable flip angle of (a) 5^0 and (b) 25^0.

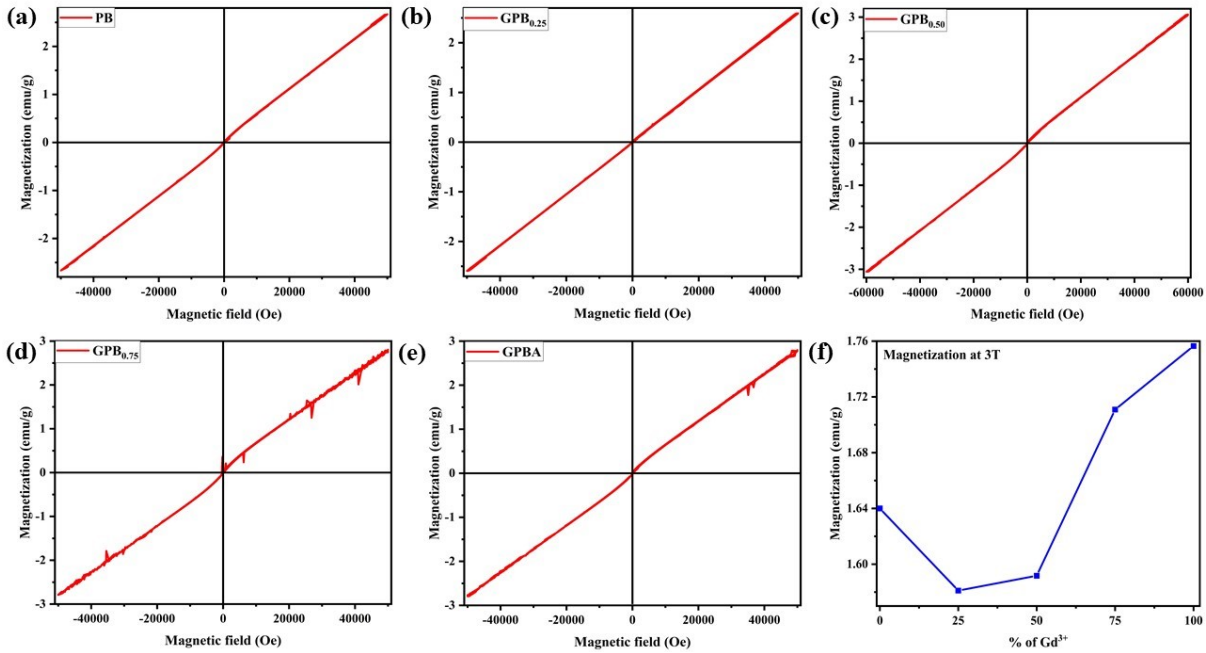

Fig. S9: SQUID magnetometry. Isothermal magnetization as a function of field at 300 K for (a) PB, (b) $GPB_{0.25}$, (c) $GPB_{0.50}$, (d) $GPB_{0.75}$ and (e) GPBA nanocubes sample. (f) Magnetization at 3T as a function of different Gd^{3+} doping in PB nanocubes at 300 K.

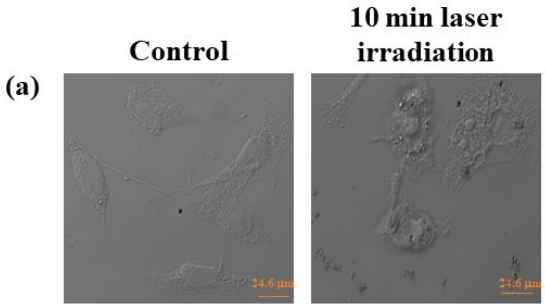

Fig. S10: (a) CLSM bright field image showing the induction of cell membrane disruption and nuclear condensation by $GPB_{0.50}$@PDA@PEG@HA@Qu under 10 minute laser exposure in MDA-MB-231 cells.

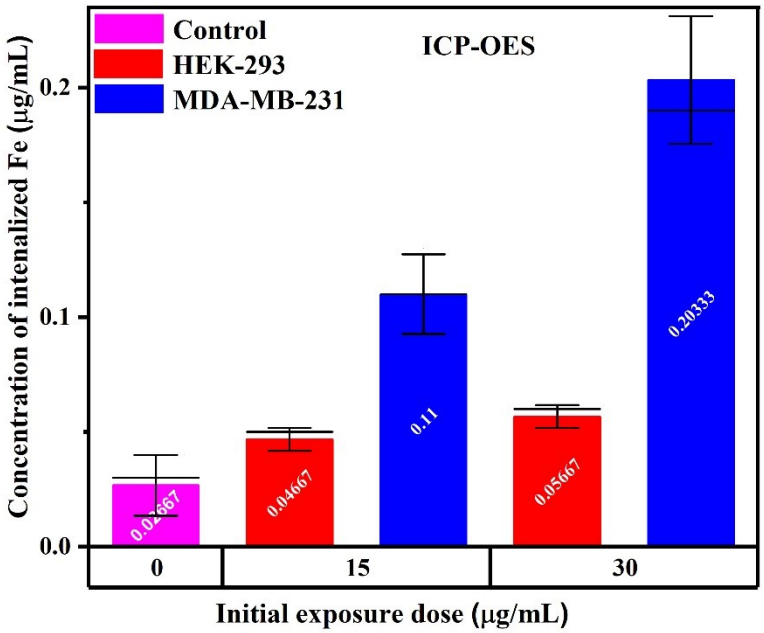

Fig. S11: ICP-OES analysis to quantify Fe uptake in HEK 293 and MDA-MB-231 cell. After 24 hr of incubation with 15 and 30 μg/mL of the $GPB_{0.50}$@PDA@PEG@HA nanocomposite, HEK 293 and MDA-MB-231 cell pellets were collected and acid digested for measurement.

Supporting information references.

1. K. C. Li, H. C. Chu, Y. Lin, H. Y. Tuan and Y. C. Hu, *ACS applied materials & interfaces*, 2016, **8**, 12082-12090.
2. Z. H. Li, Y. Chen, Y. Sun and X. Z. Zhang, *ACS nano*, 2021, **15**, 5189-5200.